RSC Advances

COMMUNICATION

View Article Online
View Journal | View Issue

Cite this: *RSC Adv.*, 2016, **6**, 47948

Received 8th April 2016
Accepted 6th May 2016

DOI: 10.1039/c6ra09108c

www.rsc.org/advances

3D Au–SiO_2 nanohybrids as a potential scaffold coating material for neuroengineering†

Paromita Kundu,*[ab] Andreea Belu,[ab] Elmar Neumann,[abc] Dirk Mayer[ab] and Andreas Offenhäusser[ab]

We demonstrate the potential application of chemically synthesized 3D Au–SiO_2 hybrid nanoparticles as a promising candidate for scaffold designing in neuroengineering. The hybrid nanospheres on substrates provide micro/nanotopography and the fine Au nanoparticles immobilized on SiO_2 spheres together provide stable adhesion cue domains facilitating adhesion and viability of the cells as well as guidance of neurites. We also investigated the cell–nanohybrid interface and interaction mechanism by FIB-SEM for a better insight into the mode of adhesion.

The nervous system forms the information processing network of a living organism where the brain acts as the centre for receiving, processing and sending out electrical signals to regulate body functions and control thought processes, expressions and actions. Neurodegenerative diseases due to ageing or at the point of injury are, therefore, serious matters of concern and a lot of research is dedicated to the development of diagnostic tools for early detection of these diseases and designing of neural implants or scaffolds for repair and regeneration of the tissues. The basic approach is to choose biocompatible substrates and their suitable surface modifications with proteins, biomolecules or appropriate ligands creates a favourable environment for the cell integration, regeneration, growth, guiding and functioning.[1] Although, the mechanisms of cell interaction and adhesion to the extracellular structures is complex and remains elusive, several studies reveal that the surface characteristics like electrostatic charges, topography, chemical nature, mechanical character, wettability are the crucial factors that controls the quality of cell adhesion or cell–chip integration, hence, the cell survival, growth and functional behaviour.[2–5] Besides, neural guiding is equally important for neurology and neural devices, from fabrication to applications. For these aspects, materials at nanoscale can offer a large range of size/shape, distribution and surface tunability to correlate with the dimension at which the cellular components work and therefore, influence neuron adhesion, growth, guiding and functionality.[6–8] For instance, the hierarchical micro/nanostructures, lithographically fabricated nanostructures[9] or template-mediated surface patterning of nanoparticles are largely used to modify flat substrates, thereby inducing the effect of surface topography in cell adhesion and for neural guiding.[10,11] By tuning the size, shape and distribution of the nanostructures on flat substrates, it is also possible to create a 3D space which leads to better understanding of the growth and networking manner of the neurons.[12–14] Au nanoparticles/structures are most promising candidates for several biomedical applications and have been largely explored in nano–neuroengineering *via* the thiol chemistry, however, the complications arise with small sized particles (<10 nm). They are more efficient candidates to promote cell adhesion but their engulfment by the cell can be cytotoxic as they can penetrate the nucleus and bind to DNA easily.[15] Here, we introduce a new strategy *i.e.* using nanohybrid structures containing the fixed smaller nanocues of Au on surface of a larger particle in order to prevent cytotoxicity. Chemically processed Au nanohybrids, particularly based on SiO_2 and graphene support, with a wide variety of composition and morphology, have been studied extensively for biosensing, bioimaging, drug delivery and therapeutics[16–18] but relatively less explored in neuroengineering. We demonstrate that the ultrafine Au nanoparticles decorated on SiO_2 spheres acts as a promising 3D nanomaterial for coating scaffolds to improve neuronal attachment, survival, growth and guiding. The cell–nanohybrid interaction is also studied in detail by FIB sectioning followed by low energy field emission scanning electron microscopy (FESEM) to gain more insight about the cell interaction mechanism with the hybrid.

In this study, we evaluate the potential of 500 nm to 1 μm sized nanohybrids consisting of SiO_2 spheres, decorated with 5–

[a]*Peter Gruenberg Institute, Bioelectronics (PGI-8), Forchungszentrum GmbH, Juelich 52425, Germany. E-mail: paro.124@gmail.com*

[b]*JARA-Fundamentals of Future Information Technology, Germany*

[c]*Helmholtz Nanoelectronic Facility (HNF), Forchungszentrum GmbH, Juelich 52425, Germany*

† Electronic supplementary information (ESI) available. See DOI: 10.1039/c6ra09108c

10 nm sized Au nanoparticles (~1400, ESI†) on the outer surface, as adhesion and guiding 3D nanocues (see ESI, Fig. S1†), where the chosen size of the hybrids was inspired from the recent report confirming the developmental acceleration of neurons with silica spheres larger than 200 nm and the effect increases with size.[19] The nanohybrid is chemically synthesized where the Au nanoparticles are synthesized by microwave chemistry, added to the silica precursor solution and left for hydrolysis to form the hybrid spheres. This results in hybrid particles with excellent stability of the Au nanoparticles on SiO_2 surface even under heating conditions of 400 °C. The Au particles were seen to be present only on the surface and strongly adherent to SiO_2, therefore, are less probable for cellular intake and toxicity. Details of the synthesis, mechanism and structural stability studies by STEM-tomography were reported recently.[20] Primary neuron cultures were used for the study and, Si and Si/SiO_2 substrates (~16 nm SiO_2 coating) were used on which the Au–SiO_2 nanospheres were dispersed randomly by spin coat (Case 1A), in line or coffee stain patterns (Case 1B) (ESI, Fig. S2†) and half coated (Case 2A & 2B) to test the influence of the hybrid on primary cortical neuron attachment, outgrowth and directionality as given in Scheme 1. The patterned substrates are fabricated by controlled dip-coating/by controlled drop casting.[21] In Case 2B, PEG-silane (see Experimental section, ESI†) was applied as the silica surface blocking agent followed by amino-thiol modification of the Au nanoparticles to promote selective cell growth. The amino-thiol binds to the Au present on SiO_2 *via* the thiol (–SH) end leaving the amine ($–NH_2$) end free for cell adhesion. Cell culture experiments were conducted on each of these samples to study the cell attachment, survival and directionality of neurites.

In Case 1A, studies were carried out on Si and Si/SiO_2 substrates to understand the impact of the surface characteristics on cell attachment. The neurons were cultured on clean Si substrates with different O_2 plasma activation duration and on Si substrates containing dispersed Au–SiO_2 hybrid particles with minimal plasma duration to ensure removal of any organic/solvent residues without alteration of the hybrid particles. After plasma activation, the surface energy, reactivity and hydrophilicity of SiO_2 increases and moreover, the dangling –OH bonds in the form of silanol groups (Si–OH) on the SiO_2 surface can favour the cell adhesion.[22,23] For Si surface too, oxygen plasma not only leads to removal of residues from Si wafer, but leads to activation of the surface by generating a thin oxide layer with silanol groups. Although, the activated SiO_2 surface might bear negative charges in the culture medium, proximity of the cell, with negatively charged membrane, to the surface can overcome the repulsive forces due the intercalating media ions and lead to the physisorption of the cell to the surface.[24] We observed a favourable attachment of neurons to the bare Si surface treated with O_2 plasma for 30 s, however, it was seen that with more days *in vitro* (DIV), *i.e.* from 3 DIV to 5 DIV, the clustering of cells increases (ESI, Fig. S3a–c†). Interestingly, an increased duration of O_2 plasma to 120 seconds improved the cell adhesion, cell singularity and growth (ESI, Fig. S3d†) of the cells but there was no striking increase in cell viability (approx. 77% for each case). In comparison, when Au–SiO_2 particles were present on the surface, even with 30 s plasma treatment, better adhesion of cells was observed without cluster formation after 3 DIV (ESI, Fig. S3f†). In terms of viability as in, the neurons present a survival percentage of 90 (approx.) on Si substrates with Au–SiO_2 hybrid particles, which was higher than the plasma treated bare Si substrates (analysis details in ESI, Fig. S3†). This shows that the favourable nature of the surface is enhanced by plasma treatment as well as on dispersing the hybrid particles on the surface, which supports the cell attachment and survival. The cell survival tested on Si/SiO_2 (~16 nm SiO_2) substrates with Au–SiO_2 shows similar results. Further studies were carried out on Si/SiO_2 substrates for 4 DIV (Fig. 1a) in order to comply with the characteristic advantages over Si substrates for future studies in general. Cell survival has also been tested with commercially available SiO_2 particles (0.5–10 μm size) dispersed on Si/SiO_2 substrates which shows 67% (approx.) viability, that is poorer than Au–SiO_2, Si and Si/SiO_2 substrates. For both types of substrates, in presence of the nanohybrid, the cells attached everywhere on the surface, however, neurites have been observed to grow towards the nanostructures. The neurites and small branching tend to extend towards the nanostructures (Fig. 1b & inset, also in ESI, Fig. S4†). The focal adhesion (FA) the neurons on the Si/SiO_2 substrates with and without hybrids nanoparticles are studied by immunostaining experiments (ESI, Experimental section†) and it shows higher FA for the substrates with hybrids as well as stronger adhesion at the hybrid particles (ESI, Fig. S5†). The neurite guidance effected by the presence of nanohybrid particles have also been evidently observed with immunostaining of the neurites. A comparative study has been performed with the commercial SiO_2 particles dispersed on Si/SiO_2 substrates and the results shows smaller FA area compared to Au–SiO_2 hybrids, however, the neurites guiding effect has been predominantly observed in this case too (ESI, Fig. S5†). The statistics obtained for the number of neurites per cell also shows higher value for the Au–SiO_2 particles than the blank Si/SiO_2 surface (ESI, Fig. S5†). Interestingly, the average length of the neurites are similar in each case, however, the mean length of the longest

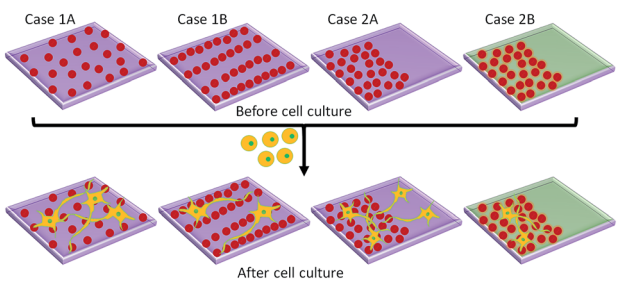

Scheme 1 Shows the different distribution of the Au–SiO_2 particles on the substrates and chemical modifications performed to understand the neuron attachment, growth and directionality. In the Cases 1A, B and 2A there was no surface modification applied except O_2 plasma activation of the Si or Si/SiO_2 surface (purple color) after dispersing the Au–SiO_2 spheres. For Case 2B, PEG-silane blocking applied on after Au–SiO_2 coating is represented by green color and further modification of the Au particles with amino-thiol is represented by orange color coating.

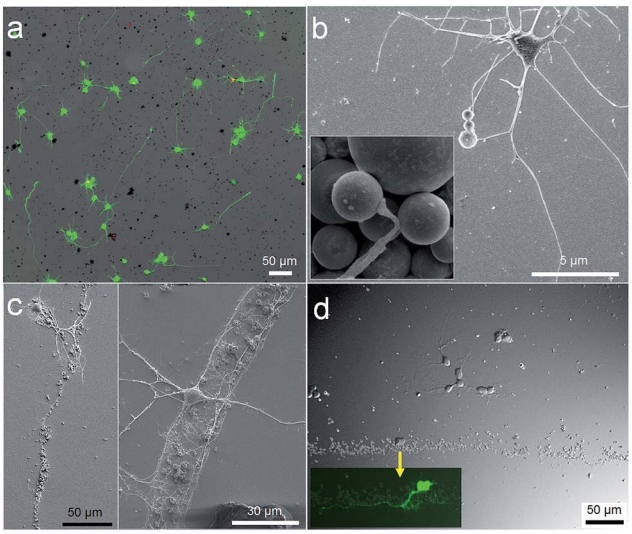

Fig. 1 (a) Fluorescence microscopy image shows the adherence and growth of neurons on the entire substrate containing Au–SiO_2 particles. (b) Low energy SEM showing the neurites extending and attaching to the nanoparticles which is more evident from the inset image that shows an outgrowth terminating on the nanohybrid. (c) SEM images show the guiding of the neurites by the random coffee stain patterns which is further prominent in (d) showing that the cells can attach anywhere on the surface, however, the neurites tend to follow the lines of nanoparticles (inset showing fluorescence microscopy image of the ROI).

neurite (axon as inferred from immunostaining) is highest (90 μm approx.) for substrates with Au–SiO_2 particles. These results can be explained by the fact that, the 3D hybrid particles in this case offers a nanotopographical modification to the surface in two length scales, firstly, due to the fine Au particles on the hybrid spheres which must be supporting the cell adhesion and survival in these cases and secondly, due to hybrid spheres themselves, contributing to the directionality/neurites guidance, which was established further from other cases as follows. In Case 1B, the cells attached to the substrate, preferably close to the bunch of nanostructures, but interestingly the neurites follow the hybrid spheres forming the coffee stain patterns (Fig. 1c) or grow towards them (more in ESI, Fig. S6†). A clear guiding effect by the nanohybrid pattern was observed in this case. This was also evident for the line patterns of Au–SiO_2 particles on Si/SiO_2 substrates as seen in different areas of substrates, given in Fig. 1d. A similar effect has been observed with the patterns of commercial SiO_2 particles (ESI, Fig. S6†), however, it was not so prominent as in case of Au–SiO_2 hybrids. Therefore, it is clear that the topography effect generated by the hybrid spheres provides guidance to the neurites. A strong adhesion of the cell soma and neurites have also been observed which resulted in the uptake of nanohybrid particles from the Si/SiO_2 surface at several locations (ESI, Fig. S6†). From these two cases, the effect of surface activation by O_2 plasma and topography is clear but the role of Au particles as chemical cues is not well understood. This obtains further clarity in the next cases. For Case 2A, where the substrate is half coated with Au–SiO_2 hybrids, the cells were seen to attach and grow in both regions, however, higher density of cells and wider networking resulted on the bare SiO_2 zone rather than the area densely coated with Au–SiO_2 (Fig. 2a and b). This could be due to the fact that a large sized aggregates of Au–SiO_2 particles (~100 μm or more) blocks the SiO_2 surface and the cells do not adhere electrostatically. The directionality of the neurites towards the nanohybrid was still observed and was prominent at the partition where the neurites from neurons on bare Si/SiO_2 surface extend towards the region containing the hybrid particles (Fig. 2c). Hence, surface topography effect is evidently present in all the cases and influences the cell adhesion as well as the direction of the outgrowths of the neurons. Case 2B clarifies the role of Au nanoparticles further where the SiO_2 surface was blocked by PEG-silane and Au nanoparticles on SiO_2 spheres were functionalized by amino-thiol. Cells do not attach on the blocked surface due to resultant protein repellent characteristics and there is normal attachment and growth of cells nanohybrid aggregates containing amino-thiol functionalized Au–SiO_2. This is obviously due to the presence of the amino groups bearing positive charges for cell attachment.[25] Besides, a specific guiding effect for cell attachment is obvious due to the chemical adhesion cues being present only on the hybrid spheres. Therefore, the neuronal attachments, outgrowths and their networking develops in the portions where the nanoparticles were arranged in line or aggregated as islands as shown in Fig. 2d and e. It is to be noted that the 3D spherical shape of the hybrid could be an additional advantage for cell adhesion as a larger number of Au particles can be present on SiO_2 sphere (about 1400 in our case), hence, higher number of adhesion cues, for a small area of point of contact of the hybrid to the blocked surface.

Finally, in each of the above cases, the adhesion is facilitated by initial electrostatic interaction with a charged surface or positive charge carrying ligand moieties followed by focal

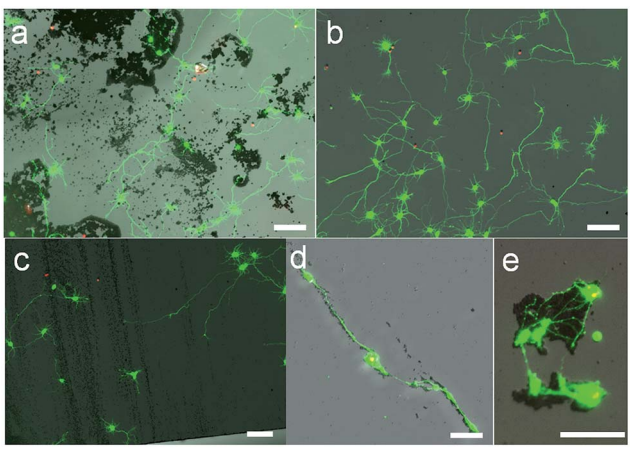

Fig. 2 Live–dead cells staining and optical images shows the adherence and growth of neurons in both the parts of the substrate, (a) with Au–SiO_2 particles and (b) without Au–SiO_2 particles but the neurites particularly extend towards the Au–SiO_2 at the partition region as seen in (c). (d and e) show more specific binding to and guidance by the Au–SiO_2 when the surrounding area is blocked by PEG-silane. The scale markers in each case denotes 100 μm.

adhesions developed under the influence of the surface topographies. The neurites growth and guidance is strongly influenced by the topography effect of the Au–SiO_2 hybrid particles where the fine Au nanoparticles on surface also acts as molecular scale tuneable chemical cues for adhesion and guiding. These factors contribute largely to the viability of the cells.

FIB sections were obtained for a further insight about the cell–nanohybrid interaction mechanism, to understand how the cells adhere to the nanostructure (see ESI, Fig. S7,† for the ROI), which is important for evaluating the nanohybrid for further applications in neural implant/chip designing. It is to be noted that the steps involved in the fixation and critical point drying procedure of the sample can lead to tension, shrinkage of the cell and hence delamination of the cell membrane from the surface as was seen in some places (ESI, marked in Fig. S7a†). Therefore, it was difficult to conclude about the quality of cell adherence to the Si/SiO_2 substrate, in spite of noticeable points of detachment of the cell membrane from the Si/SiO_2 surface (ESI, Fig. S7c†). In comparison, while analysing the portions of attachment of the cell to the Au–SiO_2 sphere, it was evident that the cell matrix wrapped around the sphere strongly unlike in the case of Si/SiO_2 substrate, and apparently engulfed the particle as in Fig. 3a. A closer look indicated a clear attachment of the cellular matrix to the Au nanoparticles on the SiO_2 spheres (Fig. 3b), but there was a thick coating of the redeposited material due to the slicing procedure. Further sectioning confirmed that the there was an attachment of the intracellular matrix to the hybrid particle from all sides and engulfed it up from the substrate at several locations. There were clear evidences of detachment of the particle from the substrate wherever the cellular matrix showed attachment to the substrate as in Fig. 3c (more in ESI, Fig. S7†). These indicated that the shape and size of the Au–SiO_2 were possibly appropriate for the uptake and also that the presence of Au nanoparticles on the silica made it a stronger cell–nanohybrid adhesion.[26] However, the uptake could also be facilitated due to the fact that the nanohybrid spheres were loosely adherent to the Si/SiO_2 surface. Cross-sections had also been obtained for a neurite interacting with the nanohybrid and it further confirmed the favourable binding interaction as in Fig. 3d.

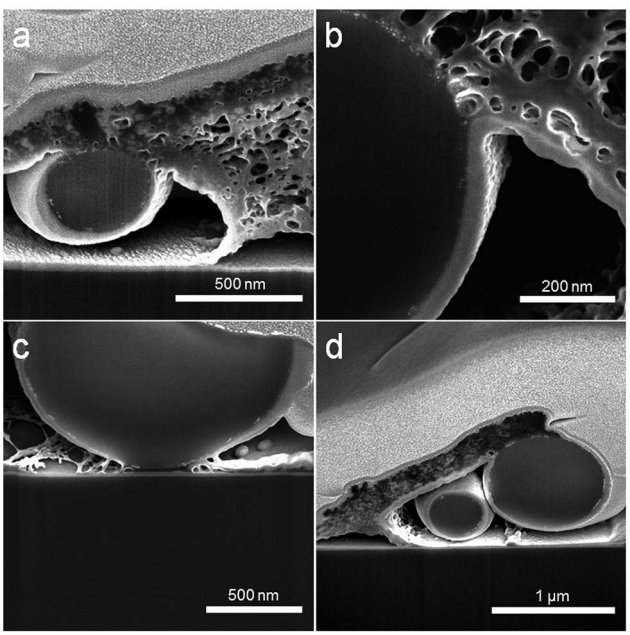

Fig. 3 SEM images of FIB sections revealing (a) interaction of cell body to the Au–SiO_2 sphere where it is engulfed by the cell (b) magnified view of the attachment of the cell matrix to the fine Au nanoparticles on SiO_2 sphere as if a portion of cell material is wrapped on the sphere (c) how the cell matrix spread on the sphere prior to complete uptake from the substrate (d) the interaction of a neurite with the nanohybrid.

Conclusions

In conclusion, the dispersion of $AuSiO_2$ hybrid spheres on a flat surface can enhance the surface characteristics by inducing nanotopography as well as chemical cues for better neuronal attachment and guiding. The ligand modification of the Au provides the attractive cues in a 3D space compared to a flat surface and this presumably offers a higher density of the adhesion points. Also the size and stability of the Au nanoparticles on SiO_2 spheres ensures its efficiency and biocompatibility, respectively, and the hybrid structure emerges as a suitable candidate for neuroengineering. We also present a basic understanding of the interaction of the neurons with the nanospheres developed by immunostaining experiments and studying the interface using FIB-SEM. It shows a strong adhesive interaction of the cell material with the Au nanoparticles, even without any ligand modification, on SiO_2 sphere surface. The cellular engulfment of the hybrid particle, observed in this case, makes it also a suitable candidate for drug delivery applications.

Acknowledgements

This research has received funding from the Helmholtz Postdoc Grant (Grant No. VH-PD-030).

References

1 K. C. Cheung, *Biomed. Microdevices*, 2007, **9**, 923–938.
2 H. G. Craighead, C. D. James and A. M. P. Turner, *Curr. Opin. Solid State Mater. Sci.*, 2001, **5**, 177–184.
3 S. S. Rao and J. Winter, *Front. Neuroeng.*, 2009, **2**, 1–14.
4 P. Roach, T. Parker, N. Gadegaard and M. R. Alexander, *Surf. Sci. Rep.*, 2010, **65**, 145–173.
5 K. Kang, M.-H. Kim, M. Park and I. S. Choi, *J. Nanosci. Nanotechnol.*, 2014, **14**, 513–521.
6 N. A. Kotov, J. O. Winter, I. P. Clements, E. Jan, B. P. Timko, S. Campidelli, S. Pathak, A. Mazzatenta, C. M. Lieber, M. Prato, R. V. Bellamkonda, G. A. Silva, N. W. S. Kam, F. Patolsky and L. Ballerini, *Adv. Mater.*, 2009, **21**, 3970–4004.
7 S. Gilles, S. Winter, K. E. Michael, S. H. Meffert, P. Li, K. Greben, U. Simon, A. Offenhäusser and D. Mayer, *Small*, 2012, **8**, 3357–3367.
8 P. Polak and O. Shefi, *Nanomedicine*, 2015, **11**, 1467–1479.
9 M. E. Spira and A. Hai, *Nat. Nanotechnol.*, 2013, **8**, 83–94.

10 J. P. Spatz and B. Geiger, in *Methods in Cell Biology*, Academic Press, 2007, vol. 83, pp. 89–111.
11 P. Li, K. Greben, R. Wordenweber, U. Simon, A. Offenhausser and D. Mayer, *RSC Adv.*, 2015, **5**, 39252–39262.
12 S. Pautot, C. Wyart and E. Y. Isacoff, *Nat. Methods*, 2008, **5**, 735–740.
13 M. Frega, M. Tedesco, P. Massobrio, M. Pesce and S. Martinoia, *Sci. Rep.*, 2014, **4**, 5489.
14 Z. Huang, Y. Sun, W. Liu, W. Zhang, W. Zheng and X. Jiang, *Small*, 2014, **10**, 2530–2536.
15 S. J. Soenen, P. Rivera-Gil, J.-M. Montenegro, W. J. Parak, S. C. De Smedt and K. Braeckmans, *Nano Today*, 2011, **6**, 446–465.
16 S. Zeng, K. V. Sreekanth, J. Shang, T. Yu, C.-K. Chen, F. Yin, D. Baillargeat, P. Coquet, H.-P. Ho, A. V. Kabashin and K.-T. Yong, *Adv. Mater.*, 2015, **27**, 6163–6169.
17 K. Turcheniuk, R. Boukherroub and S. Szunerits, *J. Mater. Chem. B*, 2015, **3**, 4301–4324.
18 L. Deng, L. Liu, C. Zhu, D. Li and S. Dong, *Chem. Commun.*, 2013, **49**, 2503–2505.
19 K. Kang, S.-E. Choi, H. S. Jang, W. K. Cho, Y. Nam, I. S. Choi and J. S. Lee, *Angew. Chem., Int. Ed.*, 2012, **51**, 2855–2858.
20 P. Kundu, H. Heidari, S. Bals, N. Ravishankar and G. Van Tendeloo, *Angew. Chem., Int. Ed.*, 2014, **53**, 3970–3974.
21 S. Watanabe, K. Inukai, S. Mizuta and M. T. Miyahara, *Langmuir*, 2009, **25**, 7287–7295.
22 T. Suni, K. Henttinen, I. Suni and J. Mäkinen, *J. Electrochem. Soc.*, 2002, **149**, G348–G351.
23 A. U. Alam, M. M. R. Howlader and M. J. Deen, *J. Micromech. Microeng.*, 2014, **24**, 035010.
24 S. Atalay, M. Barisik, A. Beskok and S. Qian, *J. Phys. Chem. C*, 2014, **118**, 10927–10935.
25 N. Schwierz, D. Horinek, S. Liese, T. Pirzer, B. N. Balzer, T. Hugel and R. R. Netz, *J. Am. Chem. Soc.*, 2012, **134**, 19628–19638.
26 H. Aviad, K. Dotan, M. Guy, E. Hadas, M. Noa, S. Joseph and E. S. Micha, *J. Neural Eng.*, 2009, **6**, 066009.